Characteristics method with cubic-spline interpolation for open channel flow computation

Tung-Lin Tsai[1,*,†,‡], Shih-Wei Chiang[2,§] and Jinn-Chuang Yang[2,¶]

[1]*Natural Hazard Mitigation Research Center, National Chiao Tung University, 1001 Ta Hsueh Road, Hsinchu, Taiwan 30010, R.O.C.*
[2]*Department of Civil Engineering, National Chiao Tung University, 1001 Ta Hsueh Road, Hsinchu, Taiwan 30010, R.O.C.*

SUMMARY

In the framework of the specified-time-interval scheme, the accuracy of the characteristic method is greatly related to the form of the interpolation. The linear interpolation was commonly used to couple the characteristics method (LI method) in open channel flow computation. The LI method is easy to implement, but it leads to an inevitable smoothing of the solution. The characteristics method with the Hermite cubic interpolation (HP method, originally developed by Holly and Preissmann, 1977) was then proposed to largely reduce the error induced by the LI method. In this paper, the cubic-spline interpolation on the space line or on the time line is employed to integrate with characteristics method (CS method) for unsteady flow computation in open channel. Two hypothetical examples, including gradually and rapidly varied flows, are used to examine the applicability of the CS method as compared with the LI method, the HP method, and the analytical solutions. The simulated results show that the CS method is comparable to the HP method and more accurate than the LI method. Without tackling the additional equations for spatial or temporal derivatives, the CS method is easier to implement and more efficient than the HP method. Copyright © 2004 John Wiley & Sons, Ltd.

KEY WORDS: characteristics method; cubic-spline interpolation; open channel flow

1. INTRODUCTION

The method of characteristics has been well known to yield many advantages on the aspects of theoretical and physical interpretation for flow pattern. This method was first used by Lai [1] and Amein [2] in the numerical modelling of unsteady flow for open channel. Later, the use of characteristics method for the unsteady flow simulation have been studied extensively

---

*Correspondence to: Tung-Lin Tsai, Natural Hazard Mitigation Research Center, National Chiao Tung University, 1001 Ta Hsueh Road, Hsinchu, Taiwan 30010, R.O.C.
†E-mail: tltsai@mail.nctu.edu.tw
‡Research Assistant Professor.
§Ph.D. student.
¶Professor.

by many researchers, such as Vardy [3], Wiggert and Sundquist [4], Wylie [5], and Goldberg and Wylie [6]. The method of characteristics could be classified into two categories. One is the characteristics-grid scheme, and the other is the specified-time-interval scheme. The characteristics-grid scheme has the potential to give accurate solution, but its grid system is awkward for practical applications. The specified-time-interval scheme then has been popular scheme for hydraulic engineering problems. With the use of the specified-time-interval scheme, characteristic trajectory usually do not pass through the grid points. The interpolation technique could be used to obtain corresponding values at the foot of the trajectory. Thus, in the framework of the specified-time-interval scheme, the form of interpolation will severely affect the accuracy of the characteristics method.

The linear interpolation was commonly used to couple characteristics method in open channel flow computation [7–10]. This method will be named as LI method in this paper. The LI method is easy to implement, but it leads to an inevitable smoothing of the solution. In order to efficiently reduce the numerical errors induced by the linear interpolation, the Hermite cubic interpolation was employed to compute unsteady flow in open channel [11]. The key to the Hermite cubic interpolation is based on the construction of cubic interpolating polynomials between the dependent variables and its derivatives for adjacent points. Holly and Preissmann [12] first combined the characteristics method with the Hermite cubic interpolation for hydraulic engineering problem. This method is usually called as HP method. The HP method with some improvements, such as the use of the characteristics reachback concept and the time line interpolation technique [13–16], had been applied to the dispersion problems. In comparison with the LI method, the HP method achieves its high accuracy at the expense of lengthy computation time for tackling auxiliary equations for spatial or temporal derivatives.

The cubic-spline interpolation, like the Hermite cubic interpolation, is another kind of piecewise cubic approximation. It is well known that the interpolation error associated with cubic splines is significantly smaller than that for Hermite cubic interpolation [17]. The cubic-spline interpolation was first used by Schohl and Holly [18] in one-dimensional advective solute transport and then applied to two-dimensional mass transport problems by Karpik and Crockett [19] and Stefanovic and Stefan [20]. The cubic-spline interpolation originally developed on the space line had also been extended to the time line [21], which allows the characteristics to intersect on the temporal axis. In this paper, the cubic-spline interpolation on the space line or on the time line is employed to integrate with characteristics method for unsteady open channel flow computation. This method will be named as CS method. It must be noticed that the HP method constructs cubic interpolating polynomials between the dependent variables and its first derivatives with respect to the time or the space for adjacent points. These first derivatives then need to be transported along the characteristics lines, which induces the additional partial differential equation to be solved. However, in the CS method, the nodal slopes are computed from the condition that a piecewise cubic interpolation should be twice continuously differentiable so that the interpolation function has a continuous curvature. Hence, the major difference between the CS method and the HP method is that the CS method need not deal with additional equations for spatial or temporal derivatives, whereas the HP method need do that. One could expect that the CS method will be easier and more efficient than the HP method. In the following sections, the mathematical and numerical formulations for the characteristics method with various interpolation techniques in modelling unsteady open channel flow are first introduced. Studies of comparisons with the LI method, the HP method,

the CS method, and the analytical solutions are then conducted on the basis of two hypothetical examples. The properties of the CS method are also demonstrated by investigation of some key parameters, such as the reachback number, the Courant number, and the weighting factor.

2. GOVERNING EQUATIONS

The well-known governing equations for one-dimensional unsteady open channel flow without lateral inflow or outflow in a uniform rectangular cross-section can be written as

$$\frac{\partial h}{\partial t} + \frac{\partial (uh)}{\partial x} = 0 \tag{1}$$

$$\frac{\partial u}{\partial t} + u\,\frac{\partial u}{\partial x} + g\,\frac{\partial h}{\partial x} = g(S_0 - S_{\mathrm{f}}) \tag{2}$$

where u is flow velocity; h is water depth; S_0 and S_{f}, respectively, denote the bed slope and friction slope; g represents the gravitational acceleration; x and t are the space and the time co-ordinates.

By introducing celerity of gravity wave, i.e. $c = \sqrt{gh}$, Equations (1) and (2) could be transformed into characteristic equations [22] as follows:

$$\frac{\mathrm{D}(u + 2c)}{\mathrm{D}t} = g(S_0 - S_{\mathrm{f}}) \tag{3}$$

along

$$\left(\frac{\mathrm{d}x}{\mathrm{d}t}\right)_{+} = u + c \tag{4}$$

and

$$\frac{\mathrm{D}(u - 2c)}{\mathrm{D}t} = g(S_0 - S_{\mathrm{f}}) \tag{5}$$

along

$$\left(\frac{\mathrm{d}x}{\mathrm{d}t}\right)_{-} = u - c \tag{6}$$

where $\mathrm{D}/\mathrm{D}t = (\partial/\partial t) + (\mathrm{d}x/\mathrm{d}t)_{\pm}(\partial/\partial t)$ denotes the total derivatives. Equations (4) and (6) represent two characteristics curves, i.e. C_+ and C_-, shown in Figure 1.
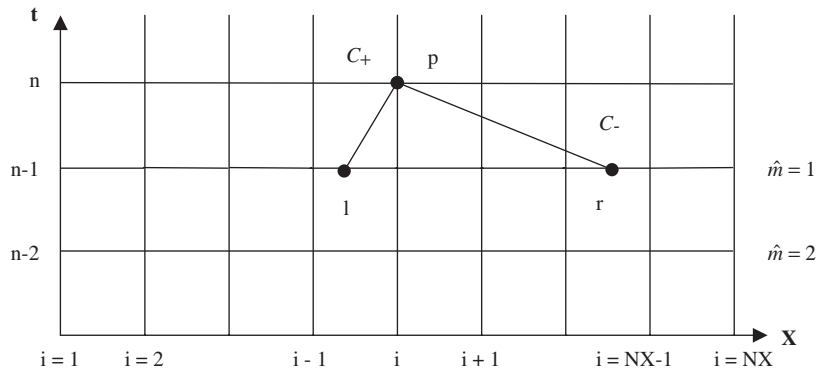
Figure 1. Grid system of characteristics method with cubic-spline interpolation.

3. NUMERICAL FRAMEWORK OF CHARACTERISTICS METHOD

3.1. Discretized equation

By integrating Equations (3)–(6) along the characteristics curves from l to p and from r to p shown in Figure 1, one can obtain

$$(u_p + 2c_p) - (u_l + 2c_l) = \int_{t_l}^{t_p} g(S_0 - S_f)\, dt \tag{7}$$

$$x_p - x_l = \int_{t_l}^{t_p} (u + c)\, dt \tag{8}$$

$$(u_p - 2c_p) - (u_r - 2c_r) = \int_{t_r}^{t_p} g(S_0 - S_f)\, dt \tag{9}$$

$$x_p - x_r = \int_{t_r}^{t_p} (u - c)\, dt \tag{10}$$

where the subscript represents the nodal point.

The time integration terms shown in right-hand sides of Equations (7)–(10) could be approximated as

$$\int_{t_l}^{t_p} \phi\, dt = \phi_{pl}(t_p - t_l) \tag{11}$$

$$\int_{t_r}^{t_p} \phi\, dt = \phi_{pr}(t_p - t_r) \tag{12}$$

where ϕ can be u, c, S_0, or S_f. The double subscript denotes a linear combination of two nodal values on the characteristics trajectory, that is, $\phi_{pl} = \omega\phi_p + (1 - \omega)\phi_l$, $\phi_{pr} = \omega\phi_p + (1 - \omega)\phi_r$ in which ω is weighting factor and ranges between zero and unity. The weighting factor of 0.5, i.e. $\omega = 0.5$, is the so-called trapezoidal-rule approximation. The rectangular-rule approximations with explicit and fully implicit forms are used when the weighting factor are zero and unity, respectively.

The nodal points r and l usually do not coincide with the grid point. Some forms of interpolations could be applied to approximate ϕ_l and ϕ_r. Due to its simplicity and efficiency, the linear interpolation, based on the construction of linear function of dependent variable between two grid points, is commonly applied to open channel flow computation. The use of the linear interpolation to approximate ϕ_l and ϕ_r is displayed in Appendix A. In the following, a brief review of the Hermite cubic interpolation for unsteady flow computation in open channel is given first and then the methodology of the cubic-spline interpolation is described.

3.2. Brief review of Hermite cubic interpolation

The key idea of the Hermite cubic interpolation is to construct a cubic polynomial function between two grid points with the use of the dependent variable and its first derivative. When the characteristic curves (i.e. C_+ and C_-) intersect on the space line, applying the Hermite cubic interpolation could yield ϕ_l and ϕ_r as follows:

$$\phi_l = a_1 \phi_{i-\hat{n}_l-1}^{n-\hat{m}} + a_2 \phi_{i-\hat{n}_l}^{n-\hat{m}} + a_3 \phi_{xi-\hat{n}_l-1}^{n-\hat{m}} + a_4 \phi_{xi-\hat{n}_l}^{n-\hat{m}} \tag{13}$$

$$\phi_r = a_1 \phi_{i-\hat{n}_r-1}^{n-\hat{m}} + a_2 \phi_{i-\hat{n}_r}^{n-\hat{m}} + a_3 \phi_{xi-\hat{n}_r-1}^{n-\hat{m}} + a_4 \phi_{xi-\hat{n}_r}^{n-\hat{m}} \tag{14}$$

with

$$\hat{n}_l = \text{INT} \frac{(u+c)_{pl}\hat{m}\Delta t}{\Delta x} \tag{15}$$

$$\hat{n}_r = \begin{cases} \text{INT} \dfrac{(u-c)_{pr}\hat{m}\Delta t}{\Delta x} & (u-c)_{pr} > 0 \\[3mm] \text{INT} \left\{ \left[\dfrac{(u-c)_{pr}\hat{m}\Delta t}{\Delta x} \right] - 1 \right\} & (u-c)_{pr} < 0 \end{cases} \tag{16}$$

where ϕ can be u or c. $\hat{m}$ denotes reachback number shown in Figure 1. Δx and Δt are the uniform grid size and the time step, respectively. INT represents the integral portion. For example, $\text{INT}\lfloor (u-c)_{pr}\hat{m}\Delta t/\Delta x \rfloor$ is integral portion of $(u-c)_{pr}\hat{m}\Delta t/\Delta x$. The coefficients $a_1 - a_4$ given by Equations (13) and (14) are shown in Appendix B.

Two additional equations are required to evaluate the spatial derivatives for flow velocity and celerity, i.e. u_x and c_x, appearing in Equations (13) and (14). By taking the spatial

derivatives of Equations (3) and (5), one can obtain

$$\frac{D(u_x + 2c_x)}{Dt} = g\frac{\partial(S_0 - S_f)}{\partial x} - (u_x + c_x)(u_x + 2c_x) \tag{17}$$

$$\frac{D(u_x - 2c_x)}{Dt} = g\frac{\partial(S_0 - S_f)}{\partial x} - (u_x - c_x)(u_x - 2c_x) \tag{18}$$

Equations (17) and (18) could be solved to yield u_x and c_x with following the concept similar to that in Equations (7)–(10) and applying the Hermite cubic interpolation to approximate ϕ_{xl} and ϕ_{xr} as follows:

$$\phi_{xl} = b_1\phi_{i-\hat{n}_l-1}^{n-\hat{m}} + b_2\phi_{i-\hat{n}_l}^{n-\hat{m}} + b_3\phi_{xi-\hat{n}_l-1}^{n-\hat{m}} + b_4\phi_{xi-\hat{n}_l}^{n-\hat{m}} \tag{19}$$

$$\phi_{xr} = b_1\phi_{i-\hat{n}_r-1}^{n-\hat{m}} + b_2\phi_{i-\hat{n}_r}^{n-\hat{m}} + b_3\phi_{xi-\hat{n}_r-1}^{n-\hat{m}} + b_4\phi_{xi-\hat{n}_r}^{n-\hat{m}} \tag{20}$$

where ϕ can be u or c. The coefficients b_1-b_4 shown in Equations (19) and (20) are displayed in Appendix B.

If the ratio of Δt to Δx is too large, the characteristic curves will intersect on the time line at boundaries rather than on the space line in the interior domain shown in Figure 2. Like the use of the Hermite cubic interpolation on the space line mentioned above, the Hermite cubic interpolation could also be employed to the time line to approximate ϕ_l and ϕ_r as follows:

$$\phi_l = a_1\phi_1^{n-\hat{m}_l-1} + a_2\phi_1^{n-\hat{m}_l} + a_3\phi_{t1}^{n-\hat{m}_l-1} + a_4\phi_{t1}^{n-\hat{m}_r} \tag{21}$$

$$\phi_{tl} = b_1\phi_1^{n-\hat{m}_l-1} + b_2\phi_1^{n-\hat{m}_l} + b_3\phi_{t1}^{n-\hat{m}_l-1} + b_4\phi_{t1}^{n-\hat{m}_l} \tag{22}$$

$$\phi_r = a_1\phi_j^{n-\hat{m}_r-1} + a_2\phi_j^{n-\hat{m}_r} + a_3\phi_{tj}^{n-\hat{m}_r-1} + a_4\phi_{tj}^{n-\hat{m}_r} \tag{23}$$

$$\phi_{tr} = b_1\phi_j^{n-\hat{m}_r-1} + b_2\phi_j^{n-\hat{m}_r} + b_3\phi_{tj}^{n-\hat{m}_r-1} + b_4\phi_{tj}^{n-\hat{m}_r} \tag{24}$$

with

$$\hat{m}_l = \text{INT}\frac{(i-1)\Delta x}{(u+c)_{pl}\Delta t} \tag{25}$$

$$\hat{m}_r = \begin{cases} \text{INT}\dfrac{(i-1)\Delta x}{(u+c)_{pr}\Delta t} & (u-c)_{pr} > 0 \\[4mm] \text{INT}\dfrac{(i-\text{NX})\Delta x}{(u-c)_{pr}\Delta t} & (u-c)_{pr} < 0 \end{cases} \tag{26}$$

where 1 and NX denote two endpoints of grid system (i.e. the upstream boundary and the downstream boundary) shown in Figure 1. $j = 1$ for $(u-c)_{pr} > 0$; $j = \text{NX}$ for $(u-c)_{pr} < 0$. The forms of the coefficients $a_1 - a_4$ and $b_1 - b_4$ in Equations (21)–(24) are exactly the same
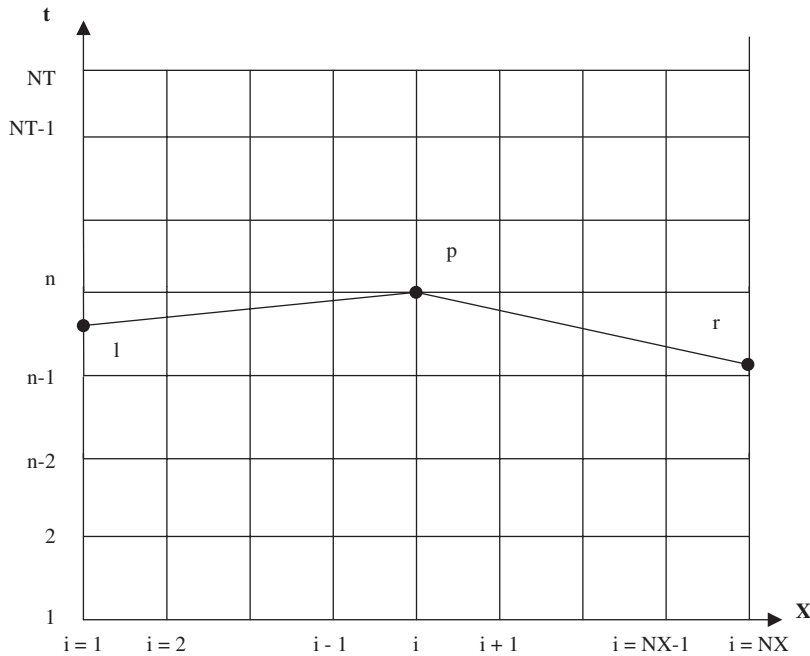
Figure 2. Grid system of characteristics method with cubic-spline interpolation at boundary.

as those in Equations (13), (14), (19) and (20). The details of the minor differences are given in Appendix B.

Like the space line interpolation, two more dependent variables u_t and c_t shown in Equations (21)–(24) could be evaluated by taking the temporal derivatives of Equations (3) and (5) as follows:

$$\frac{\mathrm{D}(u_t + 2c_t)}{\mathrm{D}t} = g\frac{\partial(S_0 - S_\mathrm{f})}{\partial t} - (u_t + c_t)(u_x + 2c_x) \tag{27}$$

$$\frac{\mathrm{D}(u_t - 2c_t)}{\mathrm{D}t} = g\frac{\partial(S_0 - S_\mathrm{f})}{\partial t} - (u_t - c_t)(u_x - 2c_x) \tag{28}$$

and employing the concept similar to that in Equations (7)–(10). However, in order to solve Equations (27) and (28), the spatial derivatives for velocity and celerity given by the last terms in right-hand sides of Equations (27) and (28) must be transformed into the temporal derivatives in advance. From Equations (1) and (2), the relations between the spatial derivatives and the temporal derivatives for flow velocity and celerity can respectively be expressed as follows:

$$u_x = \frac{u(u_t) - gu(S_0 - S_\mathrm{f}) - 2c(c_t)}{c^2 - u^2} \tag{29}$$

$$c_x = \frac{2u(c_t) - cg(S_0 - S_\mathrm{f}) - c(u_t)}{2(c^2 - u^2)} \tag{30}$$

3.3. Methodology of cubic-spline interpolation

The cubic-spline interpolation is to construct a piecewise cubic polynomial function of dependent variable between two grid points with the satisfaction of the fact that the interpolating function must pass through each given data locations (or nodes) and be continuous in its first and second derivatives at interior nodes. The cubic-spline interpolation, like the use of the Hermite cubic interpolation as mentioned above, could be applied not only to the space line but also to the time line.

When the two characteristics curves (i.e. C_+ and C_-) intersect on the space line at time level $n - \hat{m}$ shown in Figure 1, one may develop a cubic-spline interpolation function for evaluating ϕ_l and ϕ_r (ϕ could be u or c) corresponding to all the known value of ϕ at time level $n - \hat{m}$, that is, $\phi_i^{n-\hat{m}}$, $i = 1, 2, \ldots, \text{NX}$. In the cubic-spline interpolation, the second derivative of ϕ is a continuous piecewise linear function between two grid points [23, 24] as follows:

$$\phi^{n-\hat{m}}(x)'' = S_i^{n-\hat{m}} \frac{x_{i+1} - x}{\Delta x} + S_{i+1}^{n-\hat{m}} \frac{x - x_i}{\Delta x} \quad x \in [x_i, x_{i+1}] \tag{31}$$

where $i = 1, 2, \ldots, \text{NX} - 1$. $\phi^{n-\hat{m}}(x)''$ denotes the function of second derivative of ϕ at time level $n - \hat{m}$. $S_i^{n-\hat{m}}$ and $S_{i+1}^{n-\hat{m}}$ represent the second derivative of ϕ with respect to space at time level $n - \hat{m}$ and grid points i and $i + 1$, respectively. Integrating Equation (31) twice and substituting the nodal values at grid points i and $i + 1$ yields the expression for the cubic function $\phi^{n-\hat{m}}(x)$ on $[x_i, x_{i+1}]$ as follows:

$$\phi^{n-\hat{m}}(x) = S_i^{n-\hat{m}} \frac{(x_{i+1} - x)^3}{6\Delta x} + S_{i+1}^{n-\hat{m}} \frac{(x - x_i)^3}{6\Delta x} + \left(\Phi_i^{n-\hat{m}} - S_i^{n-\hat{m}} \frac{\Delta x^2}{6} \right) \frac{x_{i+1} - x}{\Delta x}$$
$$+ \left(\Phi_{i+1}^{n-\hat{m}} - S_{i+1}^{n-\hat{m}} \frac{\Delta x^2}{6} \right) \frac{x - x_i}{\Delta x} \tag{32}$$

The second derivative with respect to space at grid points shown in Equation (32) can be obtained by applying the continuity of the first derivative with respect to space at interior nodes as follows:

$$S_{i-1}^{n-\hat{m}} + 4S_i^{n-\hat{m}} + S_{i+1}^{n-\hat{m}} = \frac{6}{\Delta x^2} (\phi_{i+1}^{n-\hat{m}} - 2\phi_i^{n-\hat{m}} + \phi_{i-1}^{n-\hat{m}}) \quad i = 2, \ldots, \text{NX} - 1 \tag{33}$$

The system of Equation (33) is underdetermined as it contains only $\text{NX} - 2$ equations for finding NX unknowns. To close this system two additional constraints (i.e. two endpoint constraints) for $S_1^{n-\hat{m}}$ and $S_{\text{NX}}^{n-\hat{m}}$ are required. The frequently used natural cubic-spline interpolation simply takes $S_1^{n-\hat{m}} = S_{\text{NX}}^{n-\hat{m}} = 0$, i.e. neglect of the second derivative at endpoints [18–20], which makes the end cubics approach linearity at their extremities. Equation (33) associated with two additional endpoint constraints constructs a tridiagonal system of equations that can be easily and efficiently solved by the well-known Thomas algorithm [25].

According to the natural cubic-spline interpolation given by Equation (32) and rearranging Equation (32), ϕ_l and ϕ_r can be expressed as

$$\phi_l = A_{i-\hat{n}_l-1}^{n-\hat{m}} [(1 - \omega_l)\Delta x]^3 + B_{i-\hat{n}_l-1}^{n-\hat{m}} [(1 - \omega_l)\Delta x]^2 + C_{i-\hat{n}_l-1}^{n-\hat{m}} [(1 - \omega_l)\Delta x] + D_{i-\hat{n}_l-1}^{n-\hat{m}} \tag{34}$$

$$\phi_r = A_{i-\hat{n}_r-1}^{n-\hat{m}}[(1-\omega_r)\Delta x]^3 + B_{i-\hat{n}_r-1}^{n-\hat{m}}[(1-\omega_r)\Delta x]^2 + C_{i-\hat{n}_r-1}^{n-\hat{m}}[(1-\omega_r)\Delta x] + D_{i-\hat{n}_r-1}^{n-\hat{m}} \tag{35}$$

with

$$\omega_l = \frac{(u+c)_{pl}\hat{m}\Delta t}{\Delta x} - \hat{n}_l \tag{36}$$

$$\omega_r = \begin{cases} \dfrac{(u-c)_{pr}\hat{m}\Delta t}{\Delta x} - \hat{n}_r & (u-c)_{pr} > 0 \\[2mm] \hat{n}_r - \dfrac{(u-c)_{pr}\hat{m}\Delta t}{\Delta x} + 1 & (u-c)_{pr} < 0 \end{cases} \tag{37}$$

where $\hat{n}_l$ and $\hat{n}_r$ are given by Equations (15) and (16). The coefficients (i.e. $A_j^{n-\hat{m}}$, $B_j^{n-\hat{m}}$, $C_j^{n-\hat{m}}$, and $D_j^{n-\hat{m}}$) shown in Equations (34) and (35) can be represented as

$$A_j^{n-\hat{m}} = \frac{S_{j+1}^{n-\hat{m}} - S_j^{n-\hat{m}}}{6\Delta x} \tag{38}$$

$$B_j^{n-\hat{m}} = \frac{S_j^{n-\hat{m}}}{2} \tag{39}$$

$$C_j^{n-\hat{m}} = \frac{\phi_{j+1}^{n-\hat{m}} - \phi_j^{n-\hat{m}}}{\Delta x} - \frac{2\Delta x S_j^{n-\hat{m}} + \Delta x S_{j+1}^{n-\hat{m}}}{6} \tag{40}$$

$$D_j^{n-\hat{m}} = \phi_j^{n-\hat{m}} \tag{41}$$

where $j = 1, 2, \ldots, \text{NX} - 1$.

If the characteristics curves intersect on the time line at boundaries, i.e. the ratio of Δt to Δx is too large, the cubic-spline interpolation can be also applied to the time line. ϕ_l and ϕ_r can be approximated as

$$\phi_l = E_1^{n-\hat{m}_l-1}[(1-\zeta_l)\Delta t]^3 + F_1^{n-\hat{m}_l-1}[(1-\zeta_l)\Delta t]^2 + G_1^{n-\hat{m}_l-1}[(1-\zeta_l)\Delta t] + H_1^{n-\hat{m}_l-1} \tag{42}$$

$$\phi_r = \begin{cases} E_1^{n-\hat{m}_r-1}[(1-\zeta_r)\Delta t]^3 + F_1^{n-\hat{m}_r-1}[(1-\zeta_r)\Delta t]^2 \\ \quad + G_1^{n-\hat{m}_r-1}[(1-\zeta_r)\Delta t] + H_1^{n-\hat{m}_r-1} & (u-c)_{pr} > 0 \\[2mm] E_{\text{NX}}^{n-\hat{m}_r-1}[(1-\zeta_r)\Delta t]^3 + F_{\text{NX}}^{n-\hat{m}_r-1}[(1-\zeta_r)\Delta t]^2 \\ \quad + G_{\text{NX}}^{n-\hat{m}_r-1}[(1-\zeta_r)\Delta t] + H_{\text{NX}}^{n-\hat{m}_r-1} & (u-c)_{pr} < 0 \end{cases} \tag{43}$$

with

$$\zeta_l = \frac{(i-1)\Delta x}{(u+c)_{pl}\Delta t} - \hat{m}_l \tag{44}$$

$$
\zeta_r = \begin{cases} \dfrac{(i-1)\Delta x}{(u-c)_{pr}\Delta t} - \hat{m}_r & (u-c)_{pr} > 0 \\[2ex] \dfrac{(i-\mathrm{NX})\Delta x}{(u-c)_{pr}} - \hat{m}_r & (u-c)_{pr} < 0 \end{cases} \tag{45}
$$

The coefficients (E_j^k, F_j^k, G_j^k, and H_j^k in which j equals 1 or NX and k is $n - \hat{m}_l - 1$ or $n - \hat{m}_r - 1$) given by Equations (42) and (43), similar to those of the space line cubic-spline interpolation, are displayed in Appendix C.

Two boundary conditions and one initial condition are needed to close governing equations for the one-dimensional unsteady open channel flow shown in Equations (1) and (2). When the flow is subcritical, both the upstream boundary and downstream boundary need one condition, respectively. If the flow is supercritical, two boundary conditions must be specified at upstream boundary. The four unknowns u_p, c_p, x_r, and x_l given by Equations (7)–(10) can be solved by the two boundary conditions and initial condition with the use of the interpolation technique, such as the linear interpolation shown in Appendix A as well as the Hermite cubic interpolation and the cubic-spline interpolation mentioned above, to approximate nodal values at foot of the characteristic trajectories on the space line or on the time line.

In comparison with the use of the Hermite cubic interpolation and the cubic-spline interpolation for unsteady open channel flow computation mentioned above, one can clearly observe that the Hermite cubic interpolation needs not only to deal with the additional partial differential equations, shown in Equations (17) and (18) for space line interpolation as well as Equations (27) and (28) for time line interpolation, but also to transform the spatial derivatives of flow velocity and celerity into the temporal derivatives as shown in Equations (29) and (30). Hence, one could expect that the cubic-spline interpolation will be more efficient than the Hermite cubic interpolation. Furthermore, the cubic-spline interpolation will be easy to implement and have less complexity of coding in comparison with the Hermite cubic interpolation.

4. DEMONSTRATIONS AND EVALUATIONS

Two hypothetical examples, including gradually and rapidly varied flows, are employed to investigate the applicability of the CS method for open channel flow computation as compared with the LI method, the HP method, and the analytical solutions.

4.1. Gradually varied flow computation

A subcritical flow is assumed to take place in a rectangular prismatic channel with uniform bed slope of 0.0005 and Manning coefficient of 0.03. The channel has initial uniform flow with per unit width discharge of $q_0 = 1.0 \, \mathrm{m}^2 \, \mathrm{s}^{-1}$. The upstream boundary has an inflow discharge hydrograph of $q = q_0 + q_w[1 - \cos(2\pi t/T)]$, in which $q_w = 0.5 \, \mathrm{m}^2 \, \mathrm{s}^{-1}$ is used and T is period of time. The downstream boundary remains a uniform flow. The simulated result by the well-known Preissmann four-point scheme [26] with fine grid space is carried out to take as the basis for this comparison study. Some key parameters namely the reachback number, the Courant number, and the weighting factor are then used to demonstrate the properties of the CS method for unsteady flow computation in open channel. The channel length of 36 km and $T = 24 \, \mathrm{h}$ are used in this simulation.
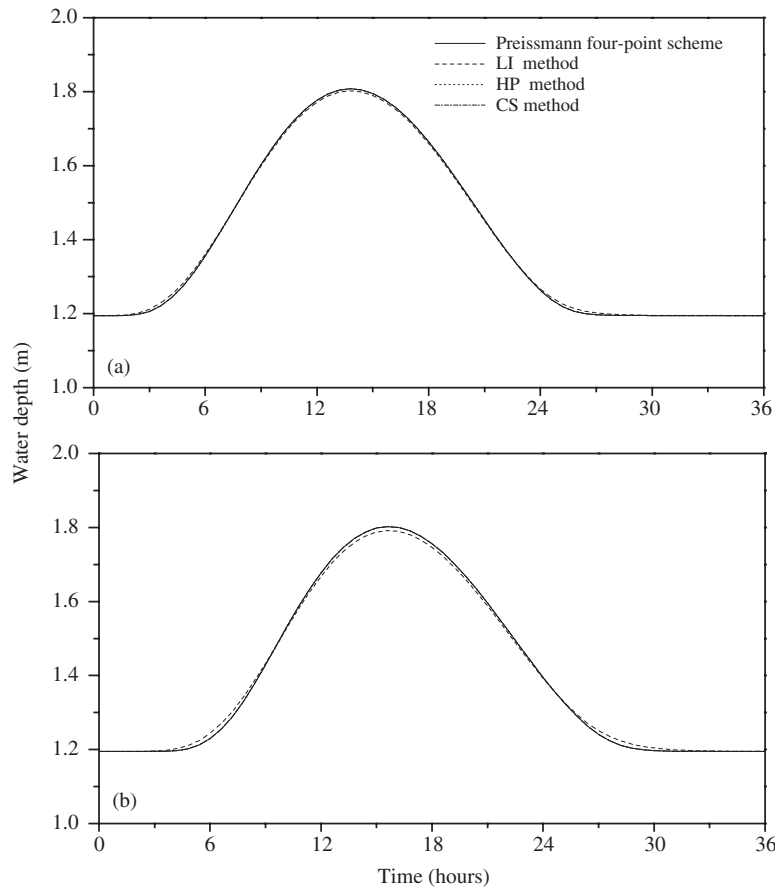
Figure 3. The change of water depth with respect to time computed from various schemes: (a) $x = 12$ km; and (b) $x = 24$ km.

Comparison study: With time step of 30 s, grid space of 1000 m, weighting factor of 0.5, and one reachback number, the simulated results in terms of the change of water depth with respect to time at the section 12 and 24 km downstream from the upstream boundary by the LI method, the HP method, and the CS method are shown in Figure 3. In Figure 3, the difference among those results computed from various methods used herein is existed but hardly to demonstrate clearly. Therefore, the relative-difference results are shown in Figure 4. The relative difference of water depth is defined as the ratio of the water depth difference between the Preissmann four-point scheme and the method used herein to the water depth by the Preissmann four-point scheme. Now one can clearly observe from Figure 4 that the HP method and the CS method have close simulated results. The LI method provides large relative differences of water depth than the CS method and the HP method. Thus, one could conclude that the HP method and the CS method are more accurate than the LI method.

Effect of reachback number: In using the characteristics method for open channel flow computation, one may be concerned with the effect of the reachback number on the accuracy
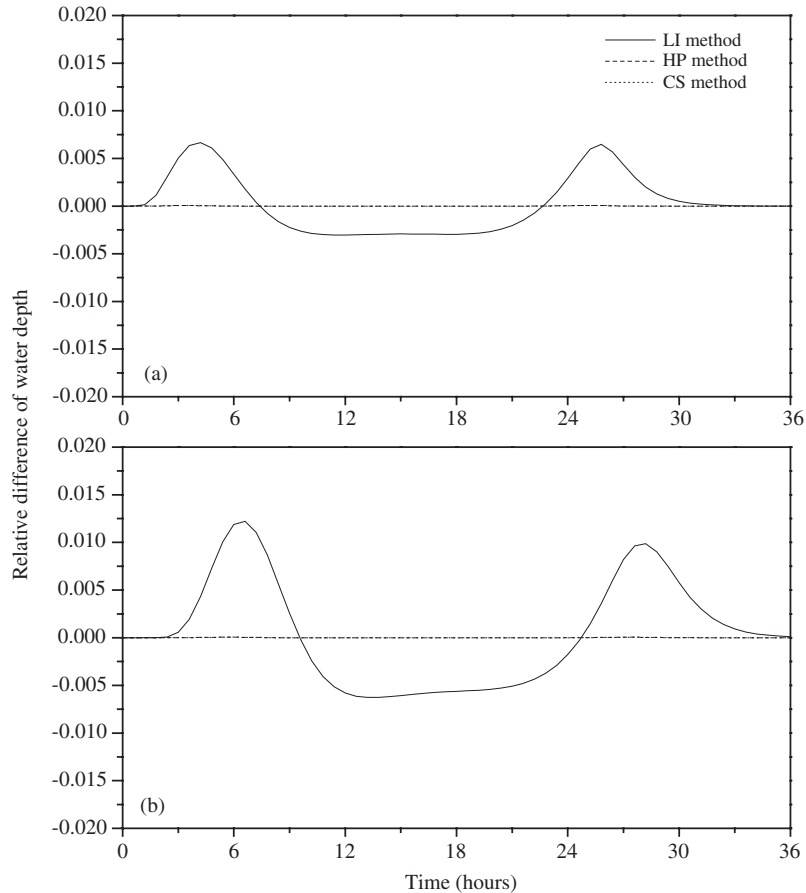
Figure 4. Relative difference of water depth with respect to time computed
from various schemes: (a) $x = 12$ km; and (b) $x = 24$ km.

of computed results. The relative difference of water depth for different reachback numbers by
the CS method, the LI method, and the HP method are displayed in Figures 5 and 6. From
Figures 5 and 6, one can observe that both the HP method and CS method have relative
differences of water depth, of order of 10^{-5}. The LI method yields relative differences of
water depth with a range of order of 10^{-3}–10^{-2}. Obviously, the LI method has large relative
differences of water depth than the CS method and the HP method. One can again find that
the CS method and the HP method have the close simulated results that are more accurate
than those by the LI method. In this case, one can know that the CS method and the HP
method seem to be insensitive to the reachback number, whereas the LI method is severely
affected by the reachback number.

The relative CPU time for different reachback numbers by the CS method, the LI method,
and the HP method are displayed in Table I. One can find from Table I that the different
reachback numbers seem not to affect the computing time. The CS method is nearly two times
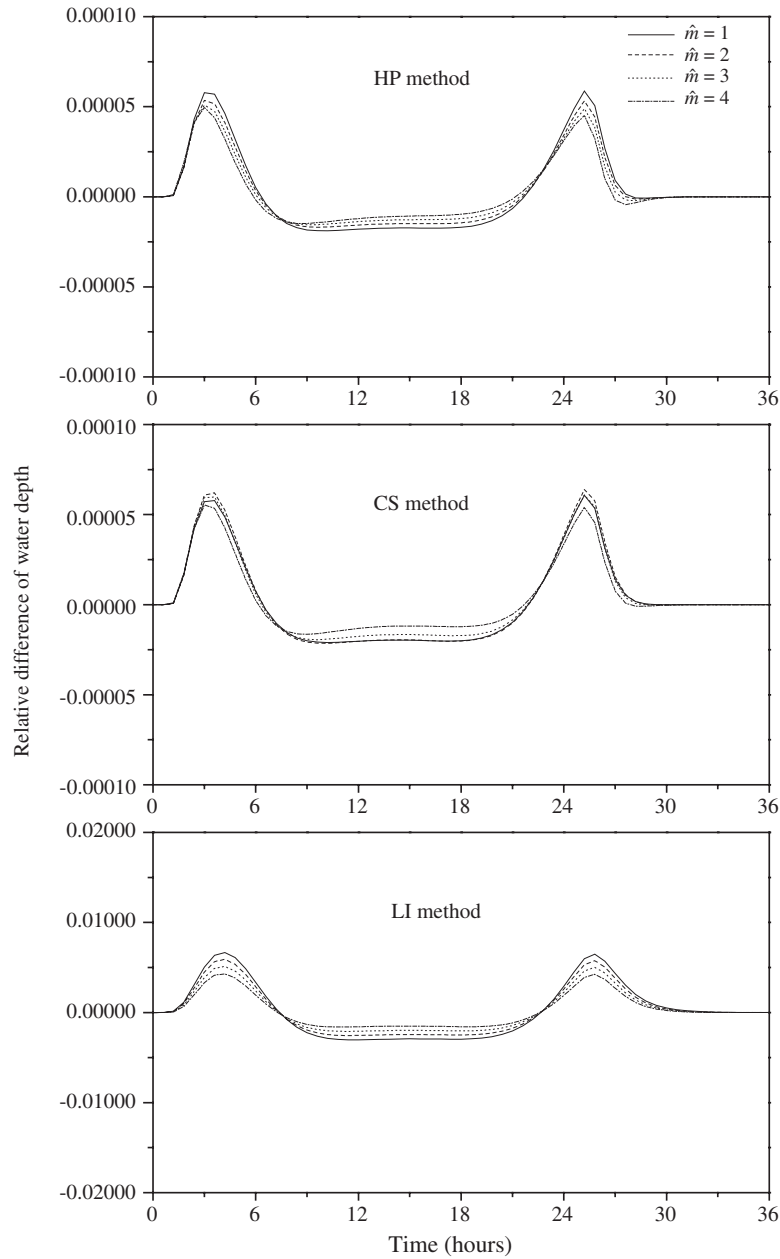
Figure 5. Relative differences of water depth computed from characteristics method with various interpolations for different reachback numbers ($x = 12$ km).
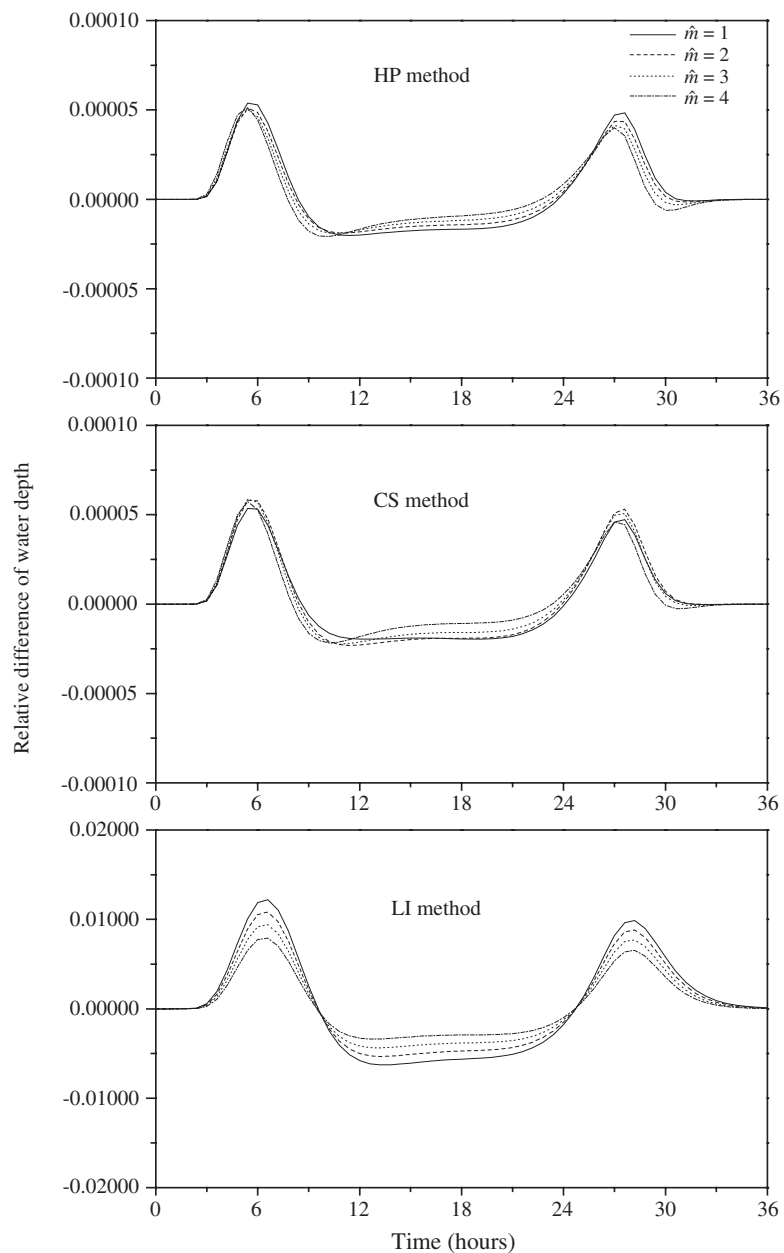
Figure 6. Relative differences of water depth computed from characteristics method with various interpolations for different reachback numbers ($x = 24$ km).

Table I. Relative CPU time of various methods with different reachback numbers.

Reachback number	LI method	HP method	CS method
1	1.00	2.23	1.92
2	1.07	2.29	1.95
3	1.01	2.30	1.95
4	1.05	2.32	1.95

the computing time of the LI method, but it consumes approximation 20% less time than the HP method. In addition, the authors also find that the CS method and the LI method are easy to implement and have less complexity of coding as compared with the HP method.

One could conclude from mentioned above that in comparison with the LI method the uses of the CS method and the HP method give more accurate simulated results. Furthermore, the HP method and the CS method are compatible. Due to the needless of tackling the additional equations for spatial and temporal derivatives, the CS method is easy to implement and more efficient than the HP method.

Effect of Courant number: In using the CS method for open channel flow computation, one of the major concern is how the Courant number influences the accuracy of simulated results. Several test runs with various time intervals have been conducted to investigate the effect of the Courant number on the accuracy of the computational results. The simulated results are shown in Figure 7. From Figure 7, one can observe that the relative differences of water depth keep in the range of order of 10^{-5}. Hence, one may conclude that the use of characteristics method with the cubic-spline interpolation for open channel flow computation is not sensitive to the Courant number. As far as the practical application is concerned, the insensitivity to the Courant number is quite an important property due to the difficulty for estimating the Courant number in the complex geometric pattern of natural river channel.

Effect of weighting factor: Due to the integration of characteristic equations along the characteristic curves, the time integration terms shown in right-hand side of Equations (7)–(10) must be evaluated. The weighting factor with respect to nodal values on the characteristic trajectory shown in Equations (11) and (12) is used to approximate the time integration term. Hence, the evaluation on how the weighting factor influences the accuracy of simulated results may be needed. Figure 8 shows the simulated results by the CS method with various weighting factors from zero to unity. From Figure 8, one can observe that the trapezoidal-rule approximation, i.e. the weighting factor of 0.5, yields the least relative difference of water depth. The weighting factor of zero and unity, i.e. rectangular-rule approximation, induce large numerical errors. This leads to conclude that the trapezoidal rule is the better choice for approximating the time integration in using the CS method for open channel flow computation.

4.2. Rapidly varied flow computation

Consider a horizontal and frictionless channel, which is 1000 m in length. A dam is located at 500 m. The initial upstream and downstream water depths are 10 and 2 m, respectively. At time $t = 0$, the dam is collapsed instantaneously.

The used computational time step is 0.25 s, and grid space is 5 m. Figure 9 shows the simulated results by the LI method, the CS method, and the HP method with one reachback
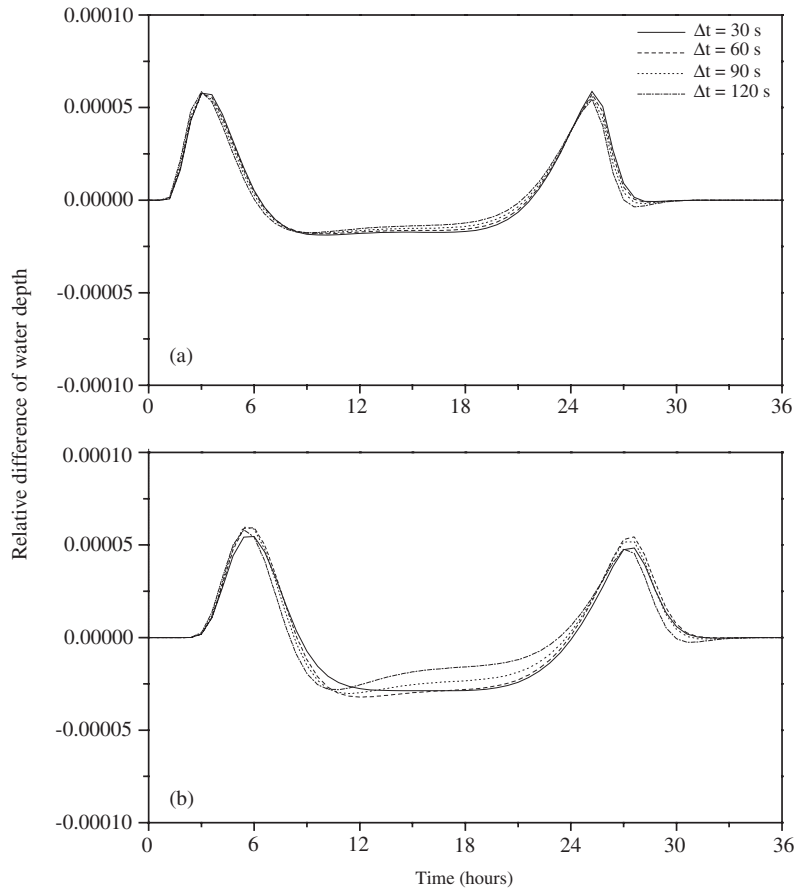
Figure 7. Relative differences of water depth computed from the CS method
with different time intervals: (a) $x = 12$ km; and (b) $x = 24$ km.

number as well as the analytical solution [27] at time $t = 30$ s after the dam failure. From
Figure 9, one can observe that the LI method produces large numerical diffusion. The CS
method and the HP method give convincing simulated results in spite of a little numerical
oscillation near the points where the derivatives of water depth are not continuous.

Table II shows the root mean square (RMS) error of water depth from various methods with
different reachback numbers. One can find from Table II that the CS method is comparable to
the HP method and more accurate than the LI method. The accuracy of the CS method, the
HP method, and the LI method increases significantly with the use of the reachback technique.
However, in the previous example of gradually varied flow where the flow pattern is quite
smooth, the simulated results by the CS method and the HP method, shown in Figures 5 and
6, have been lightly improved with the increase of the reachback number. In other words,
the LI method, the CS method, and the HP method are strongly related to the reachback
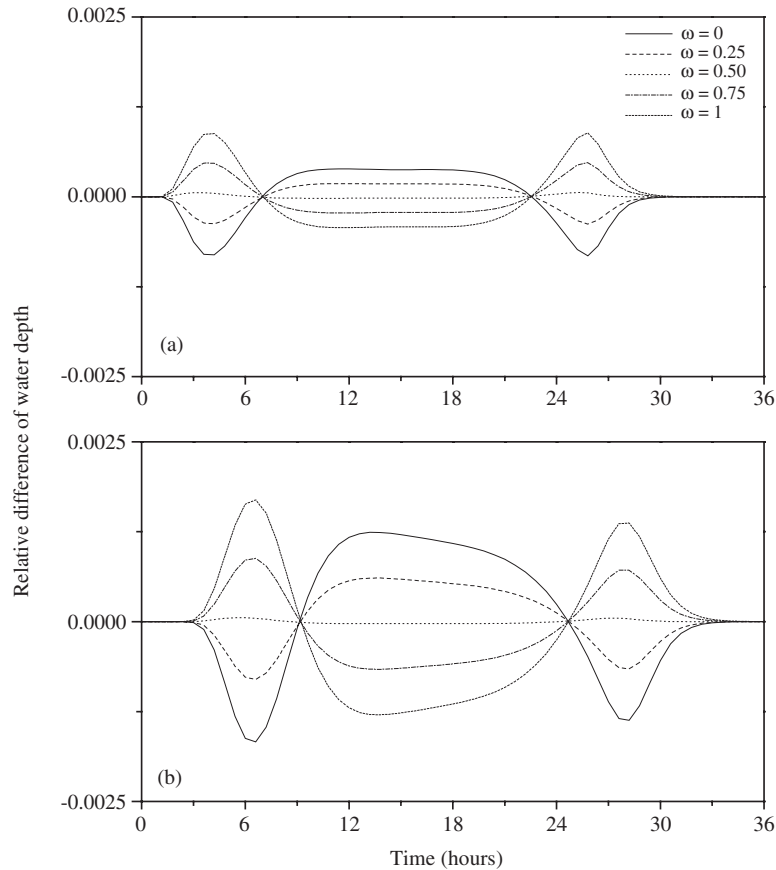number for the rapidly varied flow case, whereas the latter two methods lightly depend on

Figure 8. Relative difference of water depth computed from the CS method
with different weighting factors: (a) 12 km; and (b) 24 km.

the reachback number for the gradually varied flow case. The characteristics method with the reachback technique can indeed improve the accuracy of simulated results, especially for rapidly varied flow computation, but it may be not easy to set up initial conditions and decide reachback number for complicated open channel flows.

5. CONCLUSION

Characteristics method with the cubic-spline interpolation on the space line or on the time line (CS method) is proposed herein to compute unsteady flow in open channel. The gradually and rapidly varied flows are used to investigate the applicability of the CS method as compared with the analytical solutions as well as the LI method and the HP method, i.e. characteristics method with the linear interpolation and the Hermite cubic interpolation, respectively. The CS method and the HP method produce very close simulated results that are more accurate than
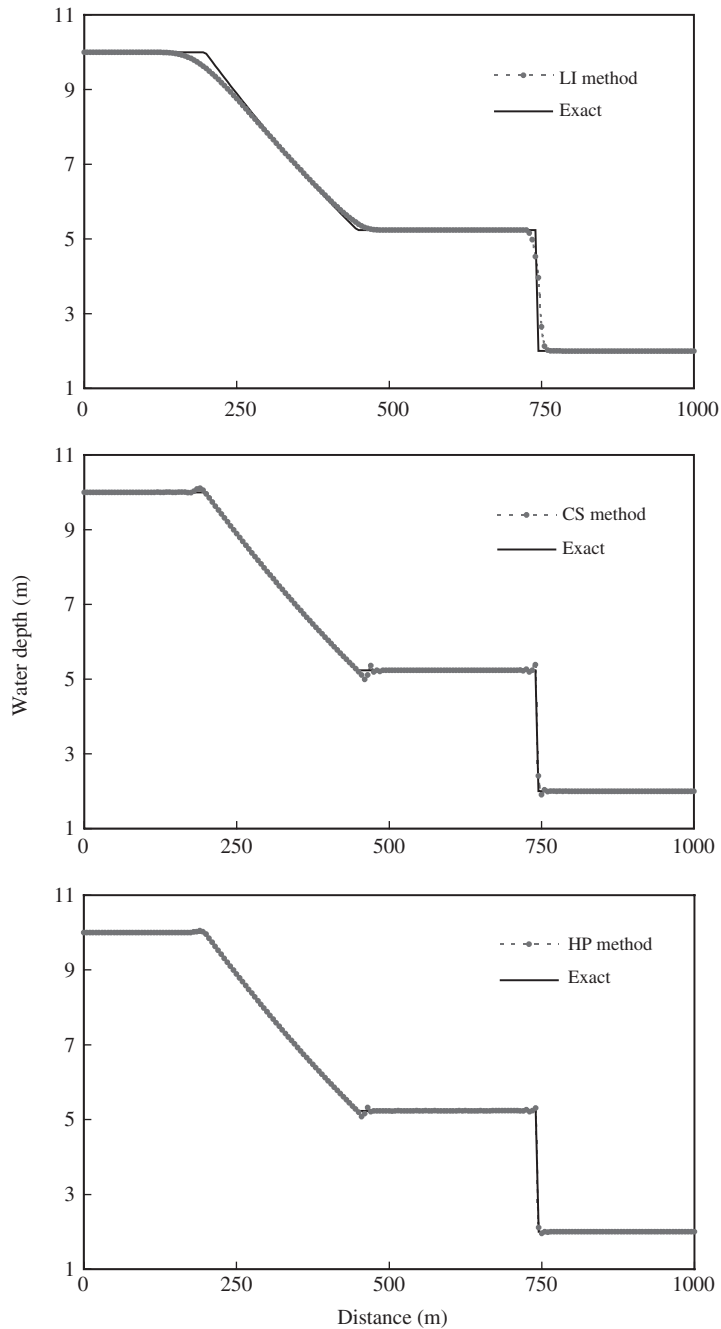
Figure 9. The simulated results of dam-break wave from various methods.

Table II. RMS error of dam-break wave simulation from various methods with different reachback numbers.

Reachback number	LI method	HP method	CS method
1	0.1698	0.0369	0.0390
2	0.0707	0.0104	0.0113
3	0.0354	0.0083	0.0092
4	0.0252	0.0076	0.0081

those by the LI method. The CS method, needing not to deal with the additional equations for spatial and temporal derivatives, is easier to implement and more efficient than the HP method. As far as accuracy, efficiency, and simplicity are concerned, the CS method, as compared with the LI method and the HP method, should be the better choice for unsteady flow computation in open channel. The accuracy of the CS method can be improved with the increase of the reachback number, especially for the rapidly varied flow case. The Courant number is insensitive to the CS method, which is quite an important property for practical applications in natural river channel. The CS method proposed herein, with the use of tensor product concept [28], can be applied to two-dimensional open channel flow computation in the further work.

APPENDIX A: CHARACTERISTICS METHOD WITH THE LINEAR INTERPOLATION

The use of the linear interpolation on the space line or on the time line to approximate ϕ_l and ϕ_r could be expressed as follows:

Space line interpolation

$$\phi_l = \omega_l \phi_{i-\hat{n}_l-1}^{n-\hat{m}} + (1 - \omega_l)\phi_{i-\hat{n}_l}^{n-\hat{m}} \tag{A1}$$

$$\phi_r = \omega_r \phi_{i-\hat{n}_r-1}^{n-\hat{m}} + (1 - \omega_r)\phi_{i-\hat{n}_r}^{n-\hat{m}} \tag{A2}$$

where ϕ could be u or c. ω_l is shown in Equation (36) and ω_r is given by Equation (37).

Time line interpolation

$$\phi_l = \zeta_l \phi_1^{n-\hat{m}_l-1} + (1 - \zeta_l)\phi_1^{n-\hat{m}_l} \tag{A3}$$

$$\phi_r = \begin{cases} \zeta_r \phi_1^{n-\hat{m}_r-1} + (1 - \zeta_r)\phi_1^{n-\hat{m}_r} & (u-c)_{pr} > 0 \\ \zeta_r \phi_{\text{NX}}^{n-\hat{m}_r-1} + (1 - \zeta_r)\phi_{\text{NX}}^{n-\hat{m}_r} & (u-c)_{pr} < 0 \end{cases} \tag{A4}$$

where ζ_l is shown in Equation (44) and ζ_r is given by Equation (45).

APPENDIX B: COEFFICIENTS OF THE HERMITE CUBIC INTERPOLATION

$$a_1 = \theta^2(3 - 2\theta) \tag{B1}$$

$$a_2 = 1 - a_1 \tag{B2}$$

$$a_3 = \theta^2(1 - \theta)\Delta x \tag{B3}$$

$$a_4 = -\theta(1 - \theta)^2\Delta x \tag{B4}$$

$$b_1 = 6\theta(\theta - 1)/\Delta x \tag{B5}$$

$$b_2 = -b_1 \tag{B6}$$

$$b_3 = \theta(3\theta - 2) \tag{B7}$$

$$b_4 = (\theta - 1)(3\theta - 1) \tag{B8}$$

In the space line interpolation, θ equals ω_l and ω_r for characteristic curve C_+ and C_-. ω_l and ω_r are shown in Equations (36) and (37), respectively. In the time line interpolation, θ equals ζ_l and ζ_r for characteristic curve C_+ and C_-. ζ_l and ζ_r are given by Equations (44) and (45), respectively. In addition, Δx need to be replaced with Δt.

APPENDIX C: COEFFICIENTS OF THE TIME LINE CUBIC-SPINE INTERPOLATION

$$E_j^k = \frac{R_j^{k+1} - R_j^k}{6\Delta t} \tag{C1}$$

$$F_j^k = \frac{R_j^k}{2} \tag{C2}$$

$$G_j^k = \frac{\phi_j^{k+1} - \phi_j^k}{\Delta t} - \frac{2\Delta t R_j^k + \Delta t R_j^{k+1}}{6} \tag{C3}$$

$$H_j^k = \phi_j^k \tag{C4}$$

where $j = 1$ or NX. $k = 1, 2, \ldots, \text{NT} - 1$ in which 1 denotes initial time level and NT represents total time level shown in Figure 2. R_j^k, second derivatives for ϕ with respect to temporal co-ordinate at grid point j and time level k, could be expressed as following relation:

$$R_j^{k-1} + 2R_j^k + R_j^{k+1} = \frac{6}{\Delta t^2}(\phi_j^{k-1} - 2\phi_j^k + \phi_j^{k+1}) \quad k = 2, 3, \ldots, \text{NT} - 1 \tag{C5}$$

According to the natural cubic-spline interpolation, two additional constraints on second derivative with respect to time at initial time level and total time level, i.e. R_j^1 and R_j^{NT},

could be represented as

$$R_j^1 = 0 \tag{C6}$$

$$R_j^{\mathrm{NT}} = 0 \tag{C7}$$

REFERENCES

1. Lai C. Flow of homogeneous density in tidal reaches, solution by the method of characteristics. *Open-file Report*, U.S. Geological Survey, Denver, CO, 1965; 65–93.
2. Amein M. Streamflow routing on computer by characteristics. *Water Resources Research* 1966; **2**:123–130.
3. Vardy AE. On the use of the method of characteristics for the solution of unsteady flows in networks. *Proceedings of 2nd International Conference on Pressure Surges*, British Hydromech. Research Association, Fluid Engineering, Cranfield, England, 1977; 15–30.
4. Wiggert DC, Sundquist MJ. Fixed-grid characteristics for pipeline transients. *Journal of Hydraulic Engineering* 1977; **103**:1403–1416.
5. Wylie EB. Inaccuracies in the characteristics method. *Proceedings of the 28th Annual Hydraulic Spec. Conference* ASCE, Chicago, IL, 1980; 165–176.
6. Goldberg DE, Wylie EB. Characteristics method using time-line interpolation. *Journal of Hydraulic Engineering* 1983; **109**:1074–1079.
7. Lai C. Numerical modeling of unsteady open channel flow. In *Advances in Hydroscience*, Chow VT, Yen BC (eds), vol. 14. Academic Press: Orlando, FL, 1986; 161–333.
8. Lai C. Comprehensive method of characteristics models for flow simulation. *Journal of Hydraulic Engineering* 1989; **114**:1074–1097.
9. Lai C. Modeling alluvial-channel flow by multimode characteristics method. *Journal of Engineering Mechanics* 1991; **117**:32–53.
10. Lai C. Multicomponent-flow analysis by multimode method of characteristics. *Journal of Hydraulic Engineering* 1994; **120**:378–395.
11. Yang JC, Chiu KP. Use of characteristics method with cubic interpolation for unsteady-flow computation. *International Journal for Numerical Methods in Fluids* 1993; **16**:329–345.
12. Holly FM Jr, Preissmann A. Accurate calculation of transport in two dimensions. *Journal of Hydraulic Engineering* 1977; **103**:1259–1277.
13. Yang JC, Hsu EL. Time-line interpolation for solution of the dispersion equation. *Journal of Hydraulic Research* 1990; **28**:503–520.
14. Yang JC, Chen KN, Lee HY. Investigation of use of reachback characteristics method for 2d dispersion equation. *International Journal for Numerical Methods in Fluids* 1991; **13**:841–855.
15. Yang JC, Hsu EL. On the use of reachback characteristics method for calculation of dispersion. *International Journal for Numerical Methods in Fluids* 1991; **12**:225–235.
16. Yang JC, Chen KN, Lee HY. An accurate computation for rapidly varied flow in open channel. *International Journal for Numerical Methods in Fluids* 1992; **14**:361–374.
17. Prenter PM. *Splines and Variational Methods*. Wiley: New York, 1975.
18. Schohl GA, Holly FM Jr. Cubic-spline interpolation in Lagrangian advection computation. *Journal of Hydraulic Engineering* 1991; **117**:248–253.
19. Karpik SR, Crockett SR. Semi-Langrangian algorithm for two-dimensional advection–diffusion equation on curvilinear coordinate meshes. *Journal of Hydraulic Engineering* 1997; **123**:389–401.
20. Stefanovic DL, Stefan HG. Accurate two-dimensional simulation of advective–diffusion–reactive transport. *Journal of Hydraulic Engineering* 2001; **127**:728–737.
21. Ahmad Z, Kothyari UC. Time-line cubic spline interpolation scheme for solution of advection equation. *Computers and Fluids* 2001; **30**:737–752.
22. Henderson FM. *Open Channel Flow*. Macmillan: New York, 1966.
23. DeBoor C. *A Practical Guide to Spline*. Springer: New York, 1978.
24. Knott GD. *Interpolating Cubic Splines*. Birkhauser: Boston, New York, 1999.
25. Thomas LH. *Elliptic Problems in Linear Difference Equations Over a Network*. Waston Scientific Computing Laboratory: Columbia, New York, 1949.
26. Cunge JA, Holly FM, Verwey A. *Practical Aspects of Computational River Hydraulics*. Pitman: London, 1980.
27. Stoker JJ. *Water Waves*. Interscience Publications, Wiley: New York, 1957.
28. Lancaster P, Salkauskas K. Curve and Surface Fitting: An Introduction. Academic Press: San Diego, 1986.